Composite fibrous filters for nano-aerosol filtration: Pressure drop and efficiency model

D. Thomas, S. Pacault, A. Charvet, N. Bardin-Monnier, J.-C. Appert-Collin

Composite Fibrous Filters for Nano-Aerosol Filtration: Pressure Drop and Efficiency Model

Thomas D.*, Pacault S., Charvet A., Bardin-Monnier N. , Appert-Collin J.-C.

Laboratoire Réactions et Génie des Procédés, Université de Lorraine, CNRS, LRGP, F-54000 Nancy, France

*Corresponding author :
E-Mail: Dominique.Thomas@univ-lorraine.fr

ABSTRACT

A model was developed to predict the behavior of non-woven filters clogged during the filtration of nanostructured particles (i.e. agglomerates of nanometric particles). It estimates the evolution of the pressure drop and the collection efficiency during particle loading. It takes into account the filter characteristics (thickness, packing density, Davies diameter and mean fiber diameter), the particle-size distribution and the operating conditions (filtration velocity, temperature…). Only one adjustable parameter (β_o) is needed, which ranges from 0.7 to 1 times the ratio of the mean fiber diameter and the Davies' diameter of the clean filter. In comparison with experimental data, the model allows satisfactorily predicting the performances (pressure drop and efficiency) of several mono or dual layer fibrous filters during particle loading.

KEYWORDS : nanoparticle, pressure drop, efficiency, modeling, clogging, fibrous filters, composite fibrous filters

INTRODUCTION

The non-woven fibrous filters are the most commonly used separation systems in airborne particle filtration because they may offer a high filter efficiency while maintaining an acceptable pressure drop. Because of their numerous manufacturing processes (drylaid, wetlaid, airlaid or spunlaid) [1], they may exhibit very different characteristics in terms of packing density, thickness or fiber size distribution. Furthermore, the interactions between the fibrous media, the aerosol and the operating conditions (filtration velocity, humidity, temperature …) have a significant impact on the deposit structure, the efficiency and the energy expenditure. Typically, the aerosols are first collected within the filter (depth-filtration). Then the filtration mode changes from depth to surface filtration with the formation of a cake on the filter surface. During the transition between these two filtration modes, the airborne particles may be collected by either the growing cake or the filter fibers. During filtration, the pressure drop and the collection efficiency evolve with time.

In order to modify their filtration properties (to increase, for example, the filtration efficiency or the particle holding capacity), different fibrous media can be associated in series. Lots of patents on filter associations [2-5] are available in literature but few articles [6-8] describe the evolution of the filter performances during clogging.

As a consequence, it might be interesting to estimate, *a priori,* the behavior of the mono- or multilayer air filters during particle loading without resorting to expensive and time-consuming experiments. The models developed, for example, could be implemented in computing codes in order to predict the aeraulic behavior of ventilation networks during the filter clogging, to optimize the structure of a non-woven filter or to estimate its lifetime. To this end, a model based on the analogy with a capillary [9] has been developed for HEPA filters by Bourrous *et al.* [10]. In this work, the authors assume that the penetration profile in the medium depth has an exponential form which does not vary over time. This assumption is justified for HEPA filters because of the low mass of particles collected within the filter, which does not induce a large modification of the internal structure before the surface filtration. This assumption becomes more questionable for medium-efficiency filters. Recently, Leung *et al.* [7] used the same approach to describe the evolution of pressure drop during the clogging of nanofibers filters. The authors consider a formation of bridges across the capillary

opening before the full closure of the pore. They introduce two parameters (the filling factor and the geometric factor governing the lateral extent of the aerosol bridge) adjusted on the experimental pressure drop evolution. This model permits to well describe the pressure drop evolution but in no case to predict it.

Moreover, most of these models cannot be qualified as complete models since they are not able to predict both the pressure drop and efficiency evolutions during the clogging of fibrous media. Some complete models were developed in the past [11-14] but none of them deal with nanostructured airborne particles (*i.e.* agglomerates of nanometric particles). More recently, Przekop and Gradon [15] built a model based on a Lattice-Boltzmann method for the calculation of the deposition efficiency of nanoparticles on two nano- and microsized fibers. It was then extended to calculate the pressure drop and the efficiency of bilayer filter structures consisting of a nanofibrous front layer and a microfibrous backing layer. This theoretical model has the advantage of taking into account the heterogeneity of the first layer but it has not been confronted with the experimental results.

During the last decade, CFD has been increasingly used in aerosol filtration [16 - 21] but the numerical generation of a nanostructured aerosol makes this approach quite complex even infeasible without using too important computing resources. Besides, as the mesh size should be smaller than the one of the primary particle of the agglomerates, the modeling of the whole filter should require a substantial number of cells that would drastically increase both the computational time and cost.

To resume, the best approach to treat this question seems to rely on the development of a computing code based on pressure drop and efficiency models taking into account the interactions between the fibers of the filter and the collected agglomerates. In particular, the analytical model developed should estimate the pressure drop of a fibrous filter during its loading by nanostructured particles while considering the modification of its efficiency due to the particles collected both within and on the surface filter. This paper is mainly focused on this new complete model, which is described and compared with experimental results obtained for different mono and dual layer fibrous filters.

I- MODELING APPROACH

The filter is discretized in layers of varying thickness (Figure 1-a). The thickness of the first five layers is considered constant and equal to twice the Davies' diameter, while the thickness of the other layers is growing according to a geometric series (with a common ratio equal to 1.5). This approach allows limiting the number of layers and thus the computing time while favoring the first layers for which a rapid evolution of the performance is expected. During the filtration, the particles collected inside the layers are going to modify the pressure drop and the efficiency. The model takes into account this evolution by calculating the fractional efficiency and the pressure drop at each time step. It should be pointed out that the main assumption in this approach is to consider an isotropic fibrous media and a homogeneous deposit in each layer.

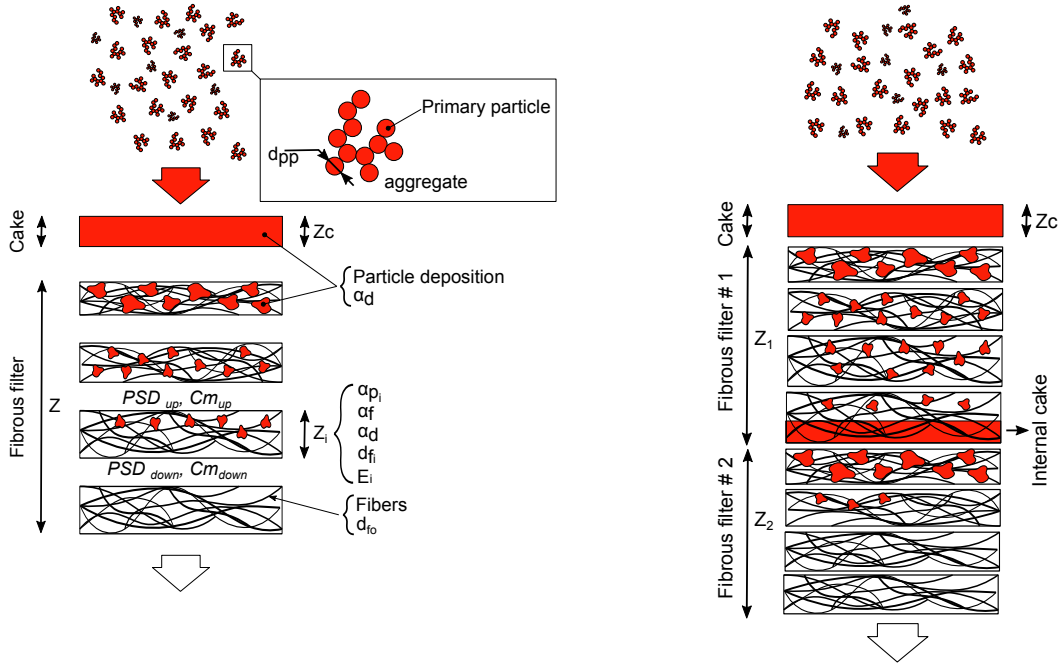

Figure 1: *Schematic diagram of filtration model*
Left) Figure 1-a : Single-layer fibrous filter – Right) Figure 1-b: Dual-layer fibrous filter

11- Pressure drop

The pressure drop of a loaded fibrous layer (before the cake formation) may be regarded as a function of the pressure drop of both the fibrous layer filter and the deposit. To consider the interactions between the fibers and the deposit, each individual pressure drop is multiplied by a factor taking into account the fiber or the deposit volume with respect to the volume and the packing density of the fibrous layer (Eq. 1). This approach is similar to the one used by Bergmann *et al.* [22] for a dendritic deposit.

$$\Delta P = \frac{\Delta Po\left(\frac{\alpha_f}{\alpha_f + \frac{\alpha_p}{\alpha_d}}\right)^{1/2} + \Delta P_d\left(\frac{\frac{\alpha_p}{\alpha_d}}{\alpha_f + \frac{\alpha_p}{\alpha_d}}\right)^{1/2}}{1 - \alpha_f - \alpha_p} \qquad \text{Eq. 1}$$

With
α_f : fiber packing density (volume of fibers / volume of fibrous layer) (-)
α_p : particle packing density (volume of collected particles / volume of fibrous layer) (-)
α_d : deposit packing density (volume of collected particles / volume of the deposit) (-)

ΔPo is the pressure drop of the clean fibrous layer which can be calculated by Davies' equation (Eq. 2).

$$\Delta Po = 64\,\frac{\alpha_f^{3/2}\left(1 + 56\alpha_f^3\right)}{d_{fo}^2\,Cu_f}\mu\,Z\,U_f \qquad \text{Eq. 2}$$

The deposit of nanostructured particles can be seen as a tangle of chains composed by juxtaposed primary particles. Thus, the pressure drop of the deposit (ΔP_d) is calculated with the Davies' equation in which the fiber diameter is replaced by the primary particle diameter (Eq 3.). It amounts to assuming the dendritic deposit with a diameter of dendrites equal to the diameter of the primary particles.

$$\Delta P_d = 64\,\frac{\alpha_p^{3/2}\left(1 + 56\alpha_p^3\right)}{d_{pp}^2\,Cu_{pp}}\mu\,Z\,U_f \qquad \text{Eq. 3}$$

With
Z: thickness of the layer considered (m)
μ : dynamic viscosity of air (Pa.s)
U_f : filtration velocity (m/s)
d_{pp} : the primary particle diameter (m)
d_{fo} : the effective fiber diameter defined by Davies [23] (clean filter) (m)
Cu_{pp}: slip correction factor (calculated with d_{pp}) (-)
Cu_f: slip correction factor (calculated with d_f) (-)

When the first layer is almost fully saturated (*i.e.* deposit volume /void volume > 0.999), the particles collected are supposed to form a cake on the filter surface, thereby contributing to an increase in the pressure drop and to the collection efficiency. The

pressure drop of the cake can be calculated by a previous model developed for nanostructured deposit [24].

$$\Delta P_G = 64\, Fc\, \frac{\alpha_d^{3/2}}{d_{pp}^2\, Cu_{pp}} \mu\, Z_C\, U_f \qquad \text{Eq. 4}$$

With
Z_c: cake thickness (m)
Fc: correction factor which takes into account the partial fusion between the primary particles. If the primary particles are in point contact, Fc is equal to 1.5.

The deposit packing density for a nanostructured deposit can be estimated from the correlation below [24] :

$$\alpha_d = 1 - \frac{1 + 0.438\, Pe}{1.019 + 0.464\, Pe} \qquad \text{Eq. 5}$$

In this expression, the Peclet number (Pe) is defined with the count median diameter of the particle size distribution.

$$Pe = \frac{CMD\ U_f}{D} \qquad \text{Eq. 6}$$

With
D: diffusion coefficient (m^2/s)
CMD : Count Median Diameter (m)

For dual layer fibrous filters in which a high efficiency filter is located downstream of a medium-efficiency filter, the formation of a cake between the two layers is also taken into account to evaluate the pressure drop and the efficiency (Figure 1-b).

12- Efficiency

The collection efficiency is estimated thanks to the correlations of the literature. Three main mechanisms have been considered: diffusion, impaction and interception (see appendix A). These models involve a uniform fiber diameter in media, which is not the case for real fibrous filters where the fiber size distribution is often polydisperse. Furthermore, during particle loading, the collection efficiency is not only linked to the fibers but also to the collected particles. So, we have considered that the collector diameter (d_C) to take into account in the different efficiency models is proportional to the effective fiber diameter (d_f) of the loaded filter which can be easily calculated from the pressure drop.

$$d_C = \beta\, d_f \qquad \text{Eq. 7}$$

The β factor is lower than or equal to 1 and as a first approximation, it has been assumed to be also a function of the Davies diameter which varies during the clogging.

$$\beta = \beta_o \left(\frac{d_{fo}}{d_f}\right)^{1/2} \qquad \text{Eq. 8}$$

Actually, β_0 must be considered as an adjusting parameter.

The effective fiber diameter is calculated from Davies' equation and the pressure drop of the layer as follows:

$$d_f = \left[64\ \frac{\left(\alpha_f + \alpha_p\right)^{3/2}\left[1 + 56\left(\alpha_f + \alpha_p\right)^3\right]}{\Delta P\, Cu_f} \eta\, Z\, U_f\right]^{1/2} \qquad \text{Eq.9}$$

Knowing the concentration and the particle size distribution upstream of the fibrous layer, for a given time step, the mass of particles collected in the layer, the concentration and the particle size distribution downstream of the fibrous layer can be calculated. The pressure drop, the Davies' diameter and the collector diameter may then be determined. The calculation procedure is repeated for all the layers including also the cake layer.

II- MATERIAL AND METHOD

The performances predicted by the model were compared to experimental results for fibrous filters (which characteristics are given in Table 1) during particle loading.

Table 1: *Properties of the filters tested*

Filter	**A**	**B**	**C**	**D**	**E**
Filter group	HEPA (H)	Medium (M)	Medium (M)	Coarse (G)	Coarse (G)
Material	Glass	PP	Glass	PET	PET
Packing density (α_f) (-)	0.076	0.050	0.074	0.241	0.217
Thickness (Z) (µm)	411	387	373	606	422
Mean diameter ($d_{f,mean}$) (µm)	0.92	2.2	5.1	26.8	16.9
Davies' diameter (d_{fo}) (µm)	1.3	4.2	6.0	34.0	19.5

PP: Polypropylene – PET: Polyethylene Terephthalate

The thickness of each filter has been determined by a laser trigonometry method inspired by Altmann and Ripperger [25] and developed by Bourrous *et al*. [10] in a previous work. The packing density may be easily deduced from the thickness, the mass per unit area of the fibrous media and the density of fibers. The mean fiber diameter was obtained by the analysis of scanning electron microscope pictures performed on about 300 fibers per filter.

The fibrous media tested is located in a filter holder of 6 cm in diameter linked to a differential pressure transmitter. These filters or association of filters were placed downstream of a spark generator (GFG1000, Palas) producing graphite nanostructured particles. This device generates a spark between two graphite electrodes under high voltage in an argon flow. The graphite material is vaporized by this spark and then condenses to form extremely tiny particles (primary particle diameter (d_{pp}) equal to 9 nm), which coagulate to form agglomerates during further transport. The primary particle size was previously determined from the association of various devices (Differential Mobility Analyzer, Aerosol Particle Mass Analyzer, Condensation Nuclei Counter) [26]. The mass concentration of particles generated was close to 1.2 mg per cubic meter.

The particle size distribution in number measured by a SMPS (Scanning Mobility Particle Sizer, nanoDMA 3085 TSI + CPC 3776 TSI) presents a count median diameter (d_{CMD}) (expressed in electrical mobility diameter) of 60 nm and a Geometric Standard Deviation (GSD) of 1.6 (Figure 2).

The mass distribution (Figure 2) is calculated from the number distribution by using the effective density ($\rho_{eff(i)}$) of the graphite nanostructured particles [26] (Eq 10).

$$\rho_{eff(i)} = 20135\ dme_i^{-1.02} \qquad \text{Eq. 10}$$

With dme_i, the electrical mobility diameter (in nm in this equation).

A control valve allows controlling the filtration airflow rate whose acquisition is insured by a flow sensor placed downstream of the filter studied. A differential pressure transducer records the filter pressure drop during particle loading.

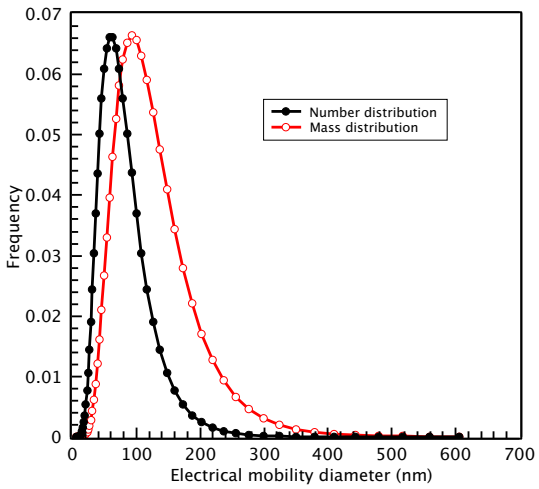

***Figure 2**: Particle size distribution in number and mass*

The number particle size distributions are frequently (every 30 minutes) measured upstream and downstream of the tested filter thanks to a SMPS to obtain the temporal evolution of fractional mass efficiency (Eq. 11).

$$E_{i,t} = \frac{Cm_{up(i,t)} - Cm_{down(i,t)}}{Cm_{up(i,t)}} \qquad \text{Eq. 11}$$

With

$$Cm_{(i,t)} = \frac{\pi\ \rho_{eff(i)}}{6}\ Cn_{(i)}\ dme_i^3 \qquad \text{Eq. 12}$$

As particle-size distributions are measured every 30 minutes, the temporal evolution of the fractional mass efficiency has been fitted by a mathematical law to calculate the collected mass by the tested filter at each time (Eq. 13).

$$Mc_t = \frac{Qv\ \Delta t}{\Omega} \sum_{dme_i} \left(\overline{Cm_{up(i)}}\ E_{i,t}\right) \qquad \text{Eq. 13}$$

With $\overline{Cm_{up(i)}}$ the mean mass concentration upstream of the filter for a given particle diameter.

The duration of each run varies from 3 to 50 hours according to the initial efficiency of the tested filter. As previously discussed [8], the deviation between calculated and weighed final collected masses is close to 10-20 % for each experiment.

III- COMPARISON WITH EXPERIMENTAL DATA

Single-layer fibrous filters

Typically, with fibrous filters, the pressure drop evolution is divided into three steps. At the beginning of the particle loading, the collection of the particles within the filter induces a slight increase of the pressure drop; this phase is called depth filtration. Then, the pressure drop is growing exponentially due to the formation of a particle

deposit on the filter surface. Some particles are still collected in the filter depth. During these two first steps, the efficiency increases with particle loading and tends toward 1. When the particle deposit is thick enough at the filter surface, all the incoming particles are collected by the deposit and the pressure drop linearly increases with the deposit thickness (surface filtration). These pressure drop and global efficiency evolutions are clearly seen on figures 3 to 8 except for the HEPA filter (filter A) for which the high initial efficiency leads quickly to surface filtration.

The figures 3 to 8 show a rather good agreement between the experimental data and the model for two filtration velocities (2.5 and 3.8 cm/s). The model describes successfully the pressure drop evolutions as well as the efficiency evolutions with the collected mass. Note that in this model the only adjustable parameter is the β_o coefficient listed in table 2 for each filter.

***Table 2**: Coefficient β_o*

Filter	**A**	**B**	**C**	**D**	**E**
β_o	0.10	0.52	0.62	1.00	0.70
$\mathbf{d_{f,mean} / d_{fo}}$	0.70	0.52	0.85	0.79	0.87

The coefficient β_o is within the range of 0.7 to 1 (df_{mean} / d_{fo}) for medium efficiency filters tested. So, as a first approximation, the coefficient β_o can be approximated by the ratio of the mean fiber diameter (df_{mean}) and the Davies' diameter of the clean filter (d_{fo}), except for the HEPA filter (filter A) for which the difference is more important (Table 2).

The model well describes that the internal clogging is all the more important that the filter has a low initial efficiency. Indeed, for the HEPA filter A (Figure 3), the pressure drop evolution is linear due to the rapid cake growth on the filter surface. Note that for this kind of filter, the efficiencies are close to 1 from the very beginning of the filtration. This is the reason why they are not represented on the figure. As expected, the collected mass of particles inside the media (before the cake formation) is even lower than the filter is initially effective (Table 3). Besides, increasing the filtration velocity tends to increase the mass collected inside the fibrous filter. Indeed, for this kind of particles, the collection is mainly governed by Brownian diffusion and the collection efficiency by this mechanism decreases with the filtration velocity. For a filter with a lower initial efficiency, the particles will be mainly located in the filter depth and consequently the cake formation will be delayed.

***Table 3:** Mass collected (g/m²) before cake formation (calculated value)*

Filter	**A**	**B**	**C**	**E**
U_f = 2.5 cm/s	0.17	0.90	1.16	2.53
Total initial efficiency @ 2.5 cm/s	≈ 1	0.75	0.6	0.54
U_f = 3.8 cm/s	0.18	1.02	1.30	-
Total initial efficiency @ 3.8 cm/s	≈ 1	0.70	0.58	-

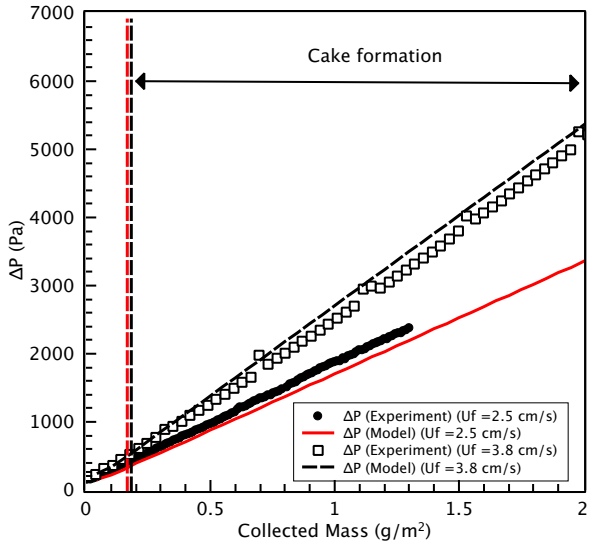

Figure 3 *: Pressure drop as a function of the collected mass*
(Filter A; filtration velocity is equal to 2.5 cm/s or 3.8 cm/s)

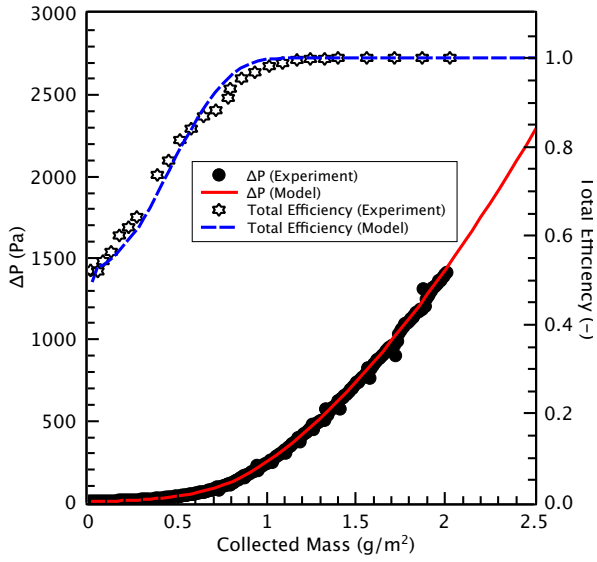

Figure 4*: Pressure drop and total efficiency as a function of the collected mass*
(Filter E; filtration velocity is equal to 2.5 cm/s)

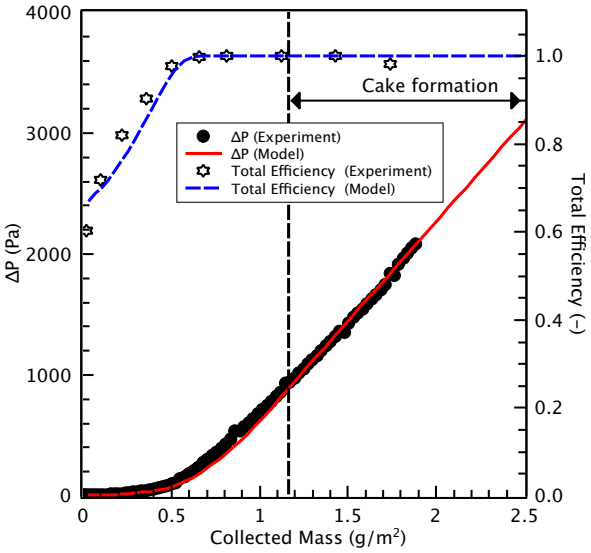

Figure 5 *: Pressure drop and total efficiency as a function of the collected mass*
(Filter C; filtration velocity is equal to 2.5 cm/s)

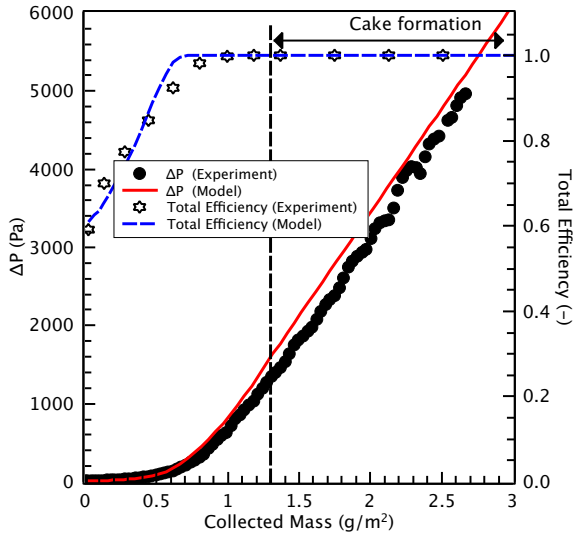

Figure 6 *: Pressure drop and total efficiency as a function of the collected mass*
(Filter C; filtration velocity is equal to 3.8 cm/s)

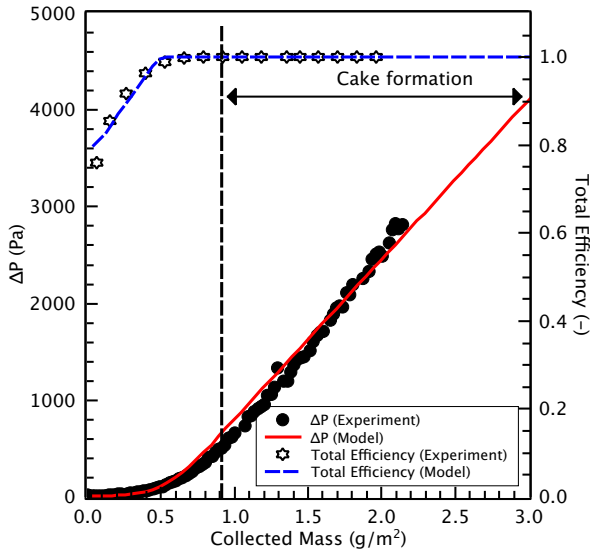

***Figure 7** : Pressure drop and total efficiency as a function of the collected mass*
(Filter B, filtration velocity is equal to 2.5 cm/s)

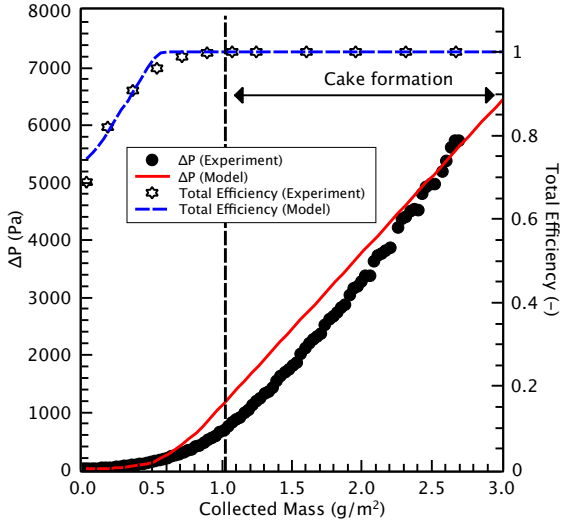

***Figure 8** : Pressure drop and total efficiency as a function of the collected mass*
(Filter B; filtration velocity is equal to 3.8 cm/s)

<u>Dual-layer fibrous filters</u>

In this configuration, a medium-efficiency filter is superimposed on the HEPA filter (Filter A). This dual-layer medium results in a collection efficiency close to 1.

Experimentally, during filtration, an internal cake may appear at the interface of the two filters when the first layer of the second filter (HEPA filter) is clogged. This internal cake continues to grow inside the last layer of the upstream filter until the upper layers become more efficient and collect all the incoming particles or until the formation of a cake at the medium-efficiency filter surface.

The figures 9 and 10 show the evolution of the modeled and experimental pressure drops during clogging for different kinds of filters associations. The global efficiency evolutions are not plotted because of the high efficiency of the composite filters, close to 1 from the beginning of the filtration. It is pointed out that for each filter, the β_o coefficients used in the model are the same as those determined previously with monolayer filter (Table 1). In other words, no additional adjustment parameter is required in these simulations with dual-layer filters.

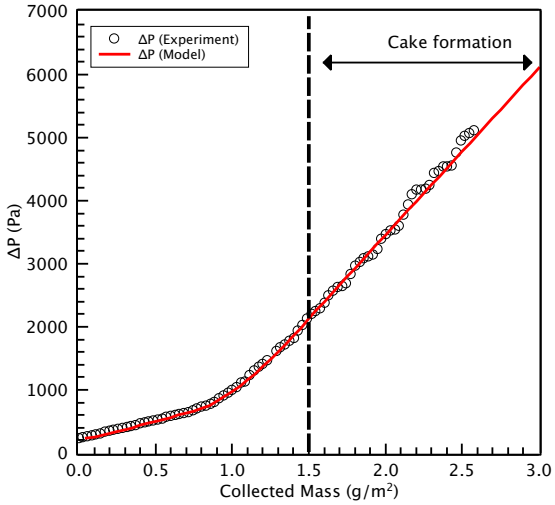

***Figure 9**: Pressure drop as a function of the collected mass*
(Filters C + A; filtration velocity is equal to 3.8 cm/s)

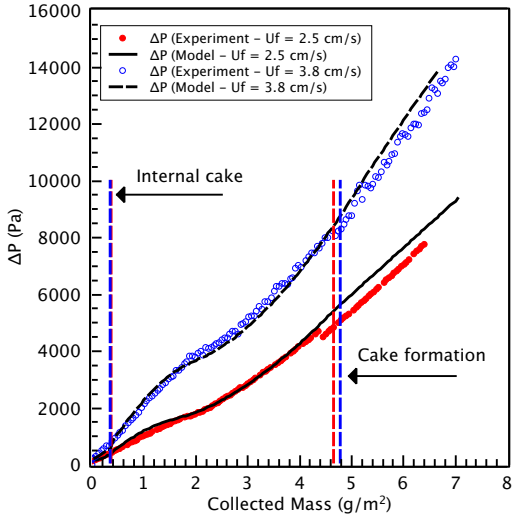

***Figure 10** : Pressure drop as a function of the collected mass*
(Filters D+A; filtration velocity is equal to 2.5 cm/s or 3.8 cm/s)

Two trends in the pressure drop evolution can be observed. The first, as for example in figure 9, shows a slow increase in pressure drop in a first step due to the particle deposit inside the first filter which is sufficiently efficient to collect a large amount of the incoming aerosol. Then, the first layer gradually clogs until forming a cake on the surface of the filter.

The second trend, as for example in figure 10, shows a quicker evolution of the pressure drop due to the internal cake formed at the surface of the HEPA because of the low efficiency of the first one. At this stage, the pressure drop is mainly governed by the internal cake. As, in diffusional regime, a filtration velocity increase induces a efficiency decrease, this shape is all the more marked that the velocity is high. Thereafter, the trend becomes similar to the one observed for the association C+A. Indeed, during filtration, the first filter becomes more and more efficient and the airborne particles are collected by the first filter until the external cake formation.

To validate our explanation, an experiment was carried out with each filter in a filter holder. Both filter holders (separated by approximatively 50-60 cm) are associated in series, the first containing the medium-efficiency filter and the second the HEPA filter (filter A). As demonstrated by Charvet *et al.* [8], the evolution of global pressure drop of the filter association is identical whatever the tested configuration (i.e. contiguous filters or filters placed in two filter holders). This configuration allows determining the particle size distributions upstream and downstream of each filter and consequently to calculate the total mass collected in each filter (Eq.13) and the mass fraction in each filter figures 11 and 12). The figure 11 confirms that a majority of the particle mass is collected by the first filter at the beginning of the particle loading. Concerning the filter D, which presents a lower initial efficiency, the particles are firstly collected at the surface of the HEPA filter (Figure 12). Subsequently, the increase of the efficiency of the first filter induces a slowing down of the pressure drop increase. Finally, when this filter reaches a global mass efficiency close to the unity, all the particles are collected within and at its surface and the formation of a cake leads to the reappearance of linear increase of pressure drop. Moreover, the model allows accurately predicting the repartition of the collected mass during particles loading.

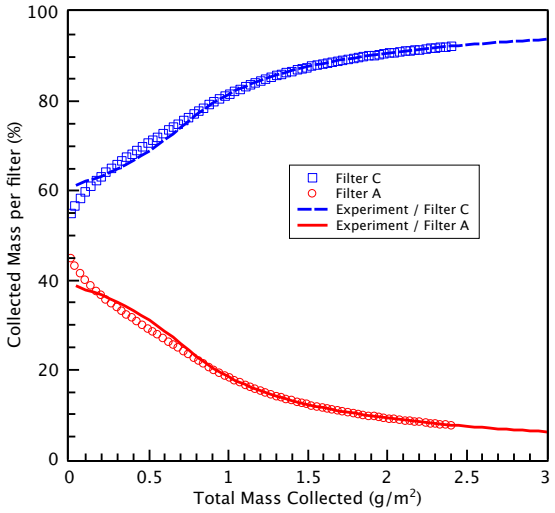

Figure 11 *: Collected Mass per filter (%) as a function of the collected mass*
(Filters C+A; filtration velocity is equal to 3.8 cm/s)

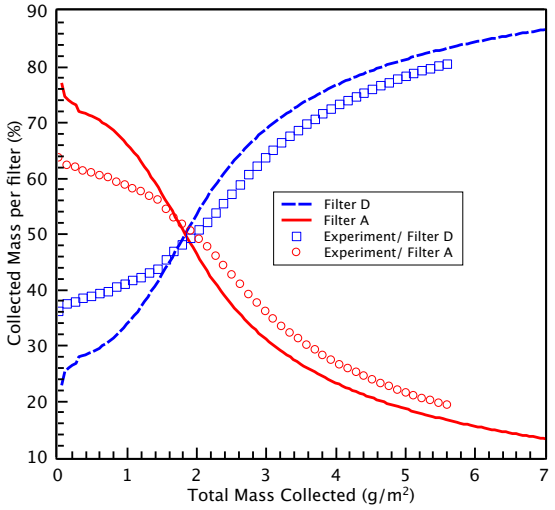

Figure 12 *: Collected Mass per filter (%) as a function of the collected mass*
(Filters D+A; filtration velocity is equal to 3.8 cm/s)

CONCLUSION

This study describes a new model estimating the evolution of the collection efficiency and pressure drop of non-woven filters clogged by nanostructured particles. The pressure drop model is based on an approach similar to the one used by Bergmann *et al.* [22]. The increase in total efficiency with particle loading is taken into account by the effective fiber diameter calculated from the pressure drop and used in the computation of the efficiency of the single fiber. This model involves only one adjustable parameter (β_o) which is within the range of 0.7 to 1 times the ratio of the mean fiber diameter (df_{mean}) and the Davies' diameter of the clean filter.

Faced with experiment data, this new model gives a good agreement for both total efficiency and pressure drop evolution. It describes very well the transition area between the depth filtration and the cake filtration.

The β_o coefficient and more generally the β factor (equation 7) must be regarded as correction factors of the single fiber collection efficiency models used which are not completely predictive because of the fiber size distribution. It must be emphasized that the β_o coefficient is only used for single fiber collection efficiency. There is not an adjustable coefficient required for determining the pressure drop. In order to improve this model, it will be necessary to study the relationship between the fiber diameter used in single fiber collection efficiency models and the fiber size distribution of the fibrous filter.

This model, applied to two filters associated in series, also gives a good agreement with experiments. It can predict the formation or not of an internal cake at the interface of the two fibrous filters. Thus, for filtration of nanostructured particles, this computing code might be interesting to use for the optimization of the structure of a fibrous filter (packing compacity, thickness, single or dual-layer).

ACKNOWLEDGMENTS

This work is a part of the LIMA joint research program between the Institut de Radioprotection et de Sûreté Nucléaire (French Institute for Radiological Protection and Nuclear Safety) and the Laboratoire Réactions et Génie des Procédés (Reactions and Chemical Engineering Laboratory).

APPENDIX A

The filtration efficiency is calculated from the well-known equation (Eq A1) below, in which the single fiber collection efficiency (η) is a function of different particle capture mechanisms.

$$E = 1 - \exp\left(-4\,\eta\,\frac{\alpha}{1-\alpha}\,\frac{Z}{\pi\,d_C}\right) \qquad \text{Eq. A-1}$$

In this approach, three main mechanisms have been considered : diffusion, inertia and interception. Considering the mechanisms as independent, the single fiber efficiency is the sum of the efficiencies related to each capture mechanism. For each mechanism, there are many expressions in the literature [27]. We have chosen three simple correlations validated by experimental data:

Inertia (Goujeon *et al*. [28])

$$\eta_I = 0.0334\ Stk^{3/2} \qquad \text{Eq. A-2}$$

With Stk (Stoke number) defined as

$$Stk = \frac{\rho_p\, d_{me}^2\, Cu_{dme}\, Uf}{9\,\mu\, d_C} \qquad \text{Eq. A-3}$$

Diffusion (Wang *et al*. [29])

$$\eta_D = 0.84\ Pe^{-0.43} \qquad \text{Eq. A-4}$$

With Pe (Peclet number) defined as

$$Pe = \frac{d_C\, Uf}{D} \qquad \text{Eq. A-5}$$

D: diffusion coefficient

This correlation has been validated in a previous work [30] on nanostructured particles.

Interception (Liu and Rubow [31])

$$\eta_{In} = 0.6\ \left(1 + 1.996\,\frac{Kn_f}{R}\right)\left(\frac{1-\alpha_{FM}}{Ku}\right)\frac{R^2}{1+R} \qquad \text{Eq. A-6}$$

With R (Interception parameter)

$$R = \frac{d_{me}}{d_C} \qquad \text{Eq. A-7}$$

d_c: collector diameter (d_f or d_{pp} as the case may be)

d_{me}: electrical mobility diameter of the airborne nanoparticles

Case of fibrous media:

$$d_C = d_f\ \ (Eq\ 9) \qquad \text{Eq. A-8}$$

$$\alpha = \alpha_f + \alpha_p \qquad \text{Eq. A-9}$$

Case of cake:

$$d_C = d_{pp} \qquad \text{Eq. A-10}$$

$$\alpha = \alpha_d\ \ (Eq\ 5) \qquad \text{Eq. A-11}$$

REFERENCES

[1] RUSSEL S.J. (2006) Handbook of Nonwovens, Elsevier Science

[2] OSENDORF R.J., Layered air filter medium having improved efficiency and pleatability, US Patent N° 5, 306, 321(1994)

[3] CHAPMAN R.L., Multilayer composite air filtration media, US Patent N° 5,419,953 (1995)

[4] BENSON J.D., CROFOOT D.G., GOGINS M.A., WEIK T.M., Filter structure with two or more layers of fine fiber having extended useful service life, US Patent N° 6,746,517 B2 (2004)

[5] RAMMIG J., SCHMIERER U., HORNFECK U., STRAUB R. Multi-layer filter structure and use of a multi-layer filter structure, US Patent N° 6,966,939 B2 (2005)

[6] WANG J., KIM S.C., PUI D.H.Y., Figure of merit of composite filters with micrometer and nanometer fibers, Aerosol Science and Technology, 42 (2008) 722-728.

[7] LEUNG W.W.F., CHOY H.-F., Transition from depth to surface filtration for a low-skin effect filter subject to continuous loading of nano-aerosols, Separation and Purification Technology, 190 (2018) 202-218

[8] CHARVET A., PACAULT S., BOURROUS S., THOMAS D., Association of fibrous filter for aerosol in predominant Brownian diffusion conditions, Separation and Purification Technology, 207 (2018) 420-426

[9] ELMOE T.D., TRICOLI A., GRUNWALDT J.-D., PRASTINIS S.E., Filtration of nanoparticles; evolution of cake structure and pressure-drop, Journal of Aerosol Science, 40 (2009) 965-981

[10] BOURROUS S., BOUILLOUX L., OUF F.-X., LEMAITRE P., NERISSON P., THOMAS D., APPERT-COLLIN J.-C., Measurement and modeling of pressure drop of HEPA filters clogged with ultrafine particles, Powder Technology, 289 (2016) 109-117

[11] LETOURNEAU P., MULCEY P., VENDEL J., Aerosol penetration inside HEPA filtration media, 21st DOE Nuclear Air Cleaning Conference (1990) 799-811

[12] LETOURNEAU P., RENAUDIN V., VENDEL J. Effects of the particle penetration inside the filter medium on the HEPA filter pressure drop, 22st DOE Nuclear Air Cleaning Conference (1992) 128-143

[13] THOMAS D., CONTAL P., V. RENAUDIN, PENICOT P., LECLERC D., VENDEL J., Modelling pressure drop in HEPA filters during dynamic filtration, Journal of Aerosol Science, Vol 30, N°2, (1999) 235-246

[14] THOMAS D., PENICOT P., CONTAL P., LECLERC D., VENDEL J., Clogging of fibrous filters by solid aerosol particles: experimental and modelling study, Chemical Engineering Science, 11, 56 (2001) 3549-3561

[15] PREZKOP R. and GRADON L., Deposition and filtration pf nanoparticles in the composites of nano- and microsized fibers, Aerosol Science and Technology, 42 (2008) 483-493

[16] QIAN F., HUANG N., ZHU X., LU J. Numerical study of the gas-solid flow characteristic of fibrous media based on SEM using CFD-DEM, Powder Technology 249 (2013) 63-70

[17] GERVAIS P.C., BOURROUS S., DANY F., BOUILLOUX L., RICCIARDI L., Simulations of filter media performances from microtomography based computational domain. Experimental and analytical comparisons, Computers and Fluids 116 (2015) 118-128.

[18] KANG S., LEE H., KIM S.-C., CHEN D-R., LIU D. Y. H., Modelling of fibrous filter media for ultrafine particle filtration, Separation and Purification Technology 209 (2019) 461-469

[19] YUE C., ZHANG Q., ZHAI Z., Numerical simulation of the filtration process in fibrous filters using CFD-DEM method, Journal of Aerosol Science 101 (2016) 174-187

[20] AZIMIAN M., KÜHNLE C., WIEGMANN A., Design and optimization of fibrous filter media using lifetime multipass simulations, Chemical Engineering and Technology, Vol 41 n°5 (2018) 1-9

[21] ILIEV O., KIRSCH R., OSTERROTH S., Combined depth and cake filtration model coupled with flow simulation for flat and pleated filters, Chemical Engineering and Technology, Vol 41 n°1 (2018) 70-78

[22] BERGMAN W., TAYLOR R.D., MILLER H.H., BIERMANN A.H., HEBARD H.D., DA ROZ R.A., LUM B.Y., Enhanced filtration program at LLL - A progress report, 15th DOE Nuclear Air Cleaning Conference (1978).

[23] DAVIES C.N., Air filtration, Academic Press, London, 1973

[24] THOMAS D., OUF F. X., GENSDARMES F., BOURROUS S., BOUILLOUX L., Pressure drop model for nanostructured deposits, Separation and Purification Technology, 138 (2014) 144—152

[25] ALTMANN J. and RIPPERGER S., Particle deposition and layer formation at the crossflow microfiltration, Journal of Membrane Science, 124 (1997) 119-128

[26] CHARVET A., BAU S., PAEZ COY N.E., BEMER D., THOMAS D., Characterizing the effective density and primary particle diameter of airborne nanoparticles produced by spark discharge using mobility and mass measurements (tandem DMA/APM), Journal of Nanoparticle Research, 16, 5 (2014) N°2418

[27] THOMAS D., CHARVET A., BARDIN- MONNIER N., APPERT-COLLIN J-C, Aerosol Filtration, ISTE edition (2017)

[28] GOUGEON R. (1994) Filtration des aérosols liquides par des filtres à fibres en régime d'interception et d'inertie, PhD Thesis, Université de Paris XII.

[29] WANG J., CHEN D.R., PUI D.Y.H., Modeling of filtration efficiency of nanoparticles in standard filter media, Journal of Nanoparticle Research, Vol 9, N°1 (2007) 109-115.

[30] MOURET G., THOMAS D., CHAZELET S., APPERT-COLLIN J.-C., BEMER D., Penetration of nanoparticles through fibrous filters perforated with defined pinholes, Journal of Aerosol Science, Vol 40, N°9 (2009) 762-775

[31] LIU B.Y.H., RUBOW K.L., Efficiency, pressure drop and figure of merit of high efficiency fibrous and membrane filter media, 5th World Filtration Congress, Vol 3 (1990) 112-119.